J. Mech. Phys. Solids Vol. 41, No. 9, pp. 1445–1459, 1993.
Printed in Great Britain.

0022–5096/93 $6.00 + 0.00

ON THE MECHANICS OF STRESS-INDUCED PHASE TRANSFORMATION IN ZIRCONIA

BERNARD BUDIANSKY and LEV TRUSKINOVSKY†

Division of Applied Sciences, Harvard University, Cambridge, MA 02138, U.S.A.; and
† Department of Aerospace Engineering and Mechanics, University of Minnesota, Minneapolis, MN 55455, U.S.A.

(*Received* 26 *February* 1993; *in revised form* 20 *May* 1993)

ABSTRACT

SOME CONSEQUENCES of a simple theoretical model for the stress-induced, isothermal phase transformation of an isolated tetragonal zirconia crystal are studied. The transformation to a monoclinic state is viewed as mechanical buckling from one homogeneous geometrical configuration to another. The model is used to predict the manner in which an applied shear stress should interact with hydrostatic stress in causing the transformation, and also the reverse monoclinic-to-tetragonal phase change. An isolated tetragonal inclusion in an elastic matrix is also considered, and its response to a far-field combination of shear and hydrostatic stress is analysed.

INTRODUCTION

THE DISCOVERY by GARVIE *et al.* (1975) of the transformation-toughening effects of zirconia (ZrO_2) particles embedded in a brittle matrix has spawned a large literature on the subject [see EVANS and HEUER (1980), EVANS and CANNON (1986), GREEN *et al.* (1989), RÜHLE and EVANS (1989) for reviews], and research continues apace. Early theoretical analyses of transformation toughening were based on the assumption that a tetragonal-to-monoclinic ($t \rightarrow m$) phase transformation of zirconia inclusions is provoked by a critical hydrostatic tension (MCMEEKING and EVANS, 1982; BUDIANSKY *et al.*, 1983), and the same basis was used in several later studies (e.g. ROSE, 1986; AMAZIGO and BUDIANSKY, 1988; STUMP and BUDIANSKY, 1989a, b). But in several theoretical studies (e.g. EVANS and CANNON, 1986; LAMBROPOULOS, 1986; CHEN and REYES MOREL, 1987; SUN *et al.*, 1990; STUMP, 1991) shear-stress effects on transformation toughening have been explored, and found to be substantial (and in Stump's work, startling). Furthermore, experiments on composites (CHEN and REYES MOREL, 1986) have shown that shear and hydrostatic stress may interact significantly in triggering the $m \rightarrow t$ transformation.

In this paper we explore some consequences of a simple Landau model for the stress-induced, isothermal phase transformation of an isolated tetragonal zirconia crystal. The transformation is viewed as mechanical buckling from one homogeneous

geometrical configuration to another. The analytical formulation is based on the most elementary polynomial strain-energy functional that is sufficiently rich to imply the t → m transformation at a critical pressure. A similar functional has been written for zirconia by CHAN (1988), but we explore its implications in rather different directions here. The model is used to predict the manner in which an applied shear stress should interact with hydrostatic stress in causing the transformation, and also the reverse m → t transformation. The theory also implies constraints on the signs and ratios of some of the elastic constants in the monoclinic phase. These results will be confronted with those of recent acoustic experiments by NEVITT *et al.* (1988) and atomic *ab initio* calculations by COHEN *et al.* (1988).

On the basis of an idealized, approximate version of the model, we also look briefly at an isolated tetragonal inclusion in an elastic matrix, and study its response to a far-field combination of shear and hydrostatic stress vis-à-vis that of an unconstrained crystal.

MODELING GOALS

Guided by various experimental observations [particularly those of BLOCK *et al.* (1985)], we shall postulate several basic phenomenological features of the phase transformations of zirconia, and attempt to build a mathematical mechanical model that is consistent with these characteristics and permits the prediction of others. We will assume that (i) at a fixed temperature a single crystal of zirconia is stable in a tetragonal configuration for sufficiently high pressures,* (ii) under *decreasing* pressure, the zirconia suddenly snaps into a homogeneous monoclinic phase (see Fig. 1) at a critical pressure $p = p_c$; and (iii) under subsequent reapplication of *increasing* pressure, a sudden reverse transformation back to the tetragonal phase occurs at $p = p_c' > p_c$. The data of BLOCK *et al.* (1985) show room-temperature values of $p_c \approx 2.8$ GPa and $p_c' = p_c + \Delta p_c \approx 3.4$ GPa during such pressure cycles, and also indicate that for increasing temperature both critical pressures decrease linearly, with Δp_c remaining constant. This hysteretic behavior is illustrated schematically by the phase diagram in pressure

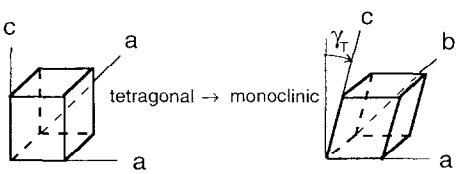

FIG. 1. Tetragonal and monoclinic axes.

*At room temperature, the high-pressure phase may really be slightly orthorhombic rather than tetragonal (ARASHI *et al.*, 1988; CHIAO and CHEN, 1990), but our elementary analysis remains applicable.

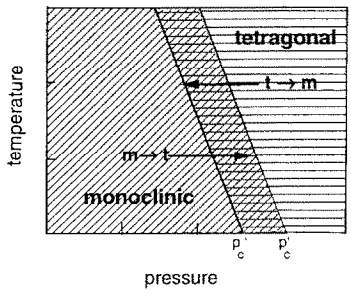

FIG. 2. Schematic pressure–temperature phase diagram.

temperature space sketched in Fig. 2, wherein the solid line represents the tetragonal-to-monoclinic (t → m) transformation under decreasing pressure at constant temperature *or* decreasing temperature at fixed pressure, and the dashed line is the m → t boundary for increasing pressure or increasing temperature. The obvious analogous interpretations of these boundaries are presumed to apply for curved paths in pressure–temperature space, but in the rest of this paper we will restrict ourselves to consideration of isothermal phase changes.

The current lore of zirconia has it that at room temperature, and under purely hydrostatic loading, a dilatational strain θ_T of about 0.04 should occur during the tetragonal-to-monoclinic phase transformation. The magnitude of the accompanying shear strain γ_T with respect to *one* of the two original pairs of *a–c* axes (see Fig. 1) is believed to be about 0.16, while the *a–a* axes, as well as the other *a–c* pair, remain orthogonal as they transform into the *a–b* and *b–c* axes in the monoclinic phase. Clearly, the transformation shear strain may be positive or negative (corresponding to symmetry related variants of monoclinic configurations) and so the sudden martensitic t → m phase change induced by decreasing pressure has the earmarks of a symmetry-breaking, mechanical instability akin to the buckling of an imperfection-sensitive structure. [The general theory of buckling and post-buckling behavior of elastic structures is due to KOITER (1945); see BUDIANSKY (1974) for a review.] Following up on this point of view, we propose to regard the t → m phase change under hydrostatic pressure as the result of a buckling instability at a critical pressure p_c that follows from an appropriately invented strain-energy functional of the dilatation θ and the shear strain γ in the *a–c* axes. The formulation should also be consistent with the hysteresis in critical pressure associated with the reverse transformation. The main goal of the exercise will then be to see—*without further assumptions or the introduction of additional adjustable parameters*—what the model would predict about the simultaneous effects of applied shear stress and pressure in provoking the t → m phase change and its reversal. Other implications of the model will also be deduced and assessed.

While this program contemplates an unconstrained zirconia single crystal, it can also be imagined applicable to a *partially stabilized* zirconia crystal containing a dopant (e.g. CaO, MgO, CeO_2, Y_2O_3) by adjustment of the magnitudes of p_c, p'_c, and if necessary, θ_T and γ_T. However, stabilization of a zirconia inclusion by surrounding elastic material is another matter, and we will use the ESHELBY (1957) equations to

make a preliminary study of the phase change of an isolated spherical zirconia inclusion in an elastic medium subjected to combined hydrostatic stress and shear. Here *twinning* becomes important, and we will make a few remarks about this.

MODEL ASSUMPTIONS AND CALCULATIONS

Strain-energy, potential energy and equilibrium

We contemplate a tetragonal crystal subjected to an applied stress, but restrict ourselves to external loading that consists only of hydrostatic stress $\sigma = -p$ and shear stress τ in a pair of a–c axes (Fig. 3), and assume that the isothermal elastic strain energy density at room temperature may be written as a smooth function $F(\theta, \gamma)$ of the associated dilatation and shear strain. Thus we suppress the possibility that a shear strain with respect to the other pair of a–c tetragonal axes will occur. Also, for convenience, we assume that $F(0,0) = 0$, and that θ is measured from the tetragonal state corresponding to $\gamma = 0$, $\sigma = \tau = 0$. The following polynomial choice for $F(\theta, \gamma)$ is the simplest one that will have the modeling consequences that we seek:

$$F(\theta,\gamma) = \tfrac{1}{2}K\theta^2 + \tfrac{1}{2}G\gamma^2 - C\theta\gamma^2 + \tfrac{1}{4}B\gamma^4 + \tfrac{1}{6}D\gamma^6. \tag{1}$$

In the conventional small-strain approximation, the specific potential energy of the loaded system is then defined by

$$\Phi = F(\theta,\gamma) - \sigma\theta - \tau\gamma \tag{2}$$

and equilibrium states (θ, γ) are governed by the conditions

$$\frac{\partial\Phi}{\partial\theta} = \frac{\partial\Phi}{\partial\gamma} = 0 \tag{3}$$

of stationary potential energy. These equilibrium states need not, of course, be stable.

Hydrostatic loading ($\tau = 0$)

With τ dropped, we get the equilibrium equations

$$K\theta - C\gamma^2 = \sigma \tag{4a}$$

$$(G - 2C\theta)\gamma + B\gamma^3 + D\gamma^5 = 0. \tag{4b}$$

The *fundamental* solution is

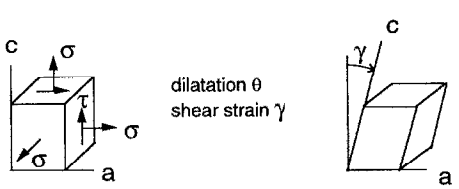

FIG. 3. Hydrostatic stress σ and shear stress τ applied to the tetragonal crystal produces dilatation θ and shear strain γ.

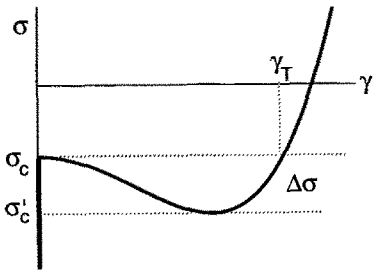

FIG. 4. Schematic relation between hydrostatic stress σ and shear strain $\gamma > 0$.

$$\theta_0 = \sigma/K, \quad \gamma_0 = 0 \tag{5}$$

which identifies K as the tetragonal bulk modulus, *which we assume to be positive.* But we require that for increasing σ (i.e. decreasing p) this solution changes from stable to unstable at some critical value of σ. Since $\partial^2\Phi/\partial\gamma^2 = G - 2C\sigma/K$ is positive when the fundamental state is stable, we must have $C > 0$, and so the tetragonal configuration becomes unstable for $\sigma > \sigma_c$ where

$$\sigma_c = -p_c = \frac{KG}{2C} \tag{6}$$

is the critical hydrostatic stress for phase transformation. Note the parameter G will be negative if the tetragonal phase is unstable in the stress-free state.

An alternative solution of (4) with $\gamma \neq 0$ is specified by

$$\theta = \frac{\sigma}{K} + \frac{C}{K}\gamma^2 \tag{7a}$$

$$\sigma - \sigma_c = \left[\frac{BK}{2C} - C\right]\gamma^2 + \left[\frac{DK}{2C}\right]\gamma^4 \tag{7b}$$

which provide σ and θ explicitly in terms of γ^2. This solution bifurcates from the fundamental one (5) at $\sigma = \sigma_c$. These equations can be put into an illuminating nondimensional form. For $\gamma > 0$, we demand that the relation between σ and γ implied by (7b) have the form sketched in Fig. 4, with a minimum at $\sigma_c' = \sigma_c - \Delta\sigma$; and (7) should have the solutions $\theta = \sigma/K + \theta_T$ and $\gamma = \gamma_T$ at $\sigma = \sigma_c$, corresponding to the monoclinic-phase strains. (There is, of course, a symmetrical solution with $\gamma < 0$.) If we eliminate the constants in (7) in favor of K, θ_T, γ_T and $\Delta\sigma$, we get

$$\begin{cases} B = 2K\left(\dfrac{\theta_T^2}{\gamma_T^4}\right) - \dfrac{8\Delta\sigma\theta_T}{\gamma_T^4} \\ C = K\left(\dfrac{\theta_T}{\gamma_T^2}\right) \\ D = \dfrac{8\Delta\sigma\theta_T}{\gamma_T^6} \end{cases} \tag{8}$$

and we can write (7) as

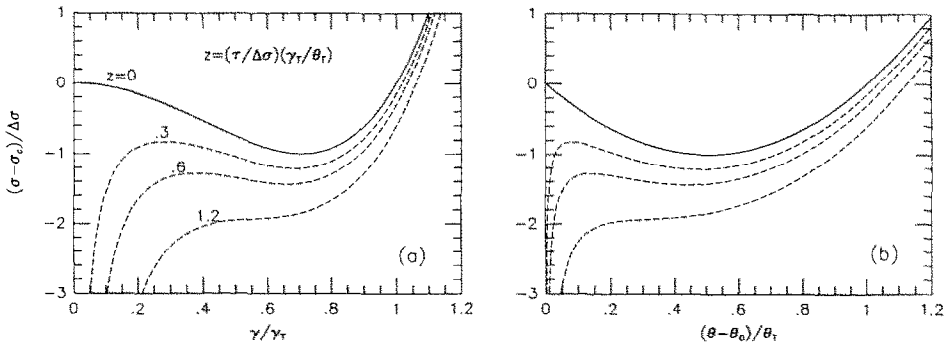

FIG. 5. Non-dimensional hydrostatic-stress change vs (a) normalized shear strain and (b) normalized dilatation change, for various values of the non-dimensional shear stress parameter z.

$$\frac{\theta-\theta_0}{\theta_T}=\left(\frac{\gamma}{\gamma_T}\right)^2 \tag{9a}$$

$$\frac{\sigma-\sigma_c}{\Delta\sigma}=4\left[-\left(\frac{\gamma}{\gamma_T}\right)^2+\left(\frac{\gamma}{\gamma_T}\right)^4\right] \tag{9b}$$

where θ_0 is the linear function of σ given in (5). These equations provide the non-dimensional relations between load and distortion shown by the solid curves in Figs 5(a) and (b). We review the behavior these curves reflect. Starting out from the tetragonal phase ($\gamma=0$) with $\sigma<\sigma_c$, increasing σ simply induces elastic dilatation changes until the martensitic phase transformation into the monoclinic state occurs as a consequence of the buckling instability at $\sigma=\sigma_c$. Then γ jumps to γ_T and θ increases suddenly by the amount θ_T. Under subsequent stress reversal, the material snaps back to the tetragonal shape when σ reaches $\sigma_c-\Delta\sigma$.

An immediate consequence of our simple model is that the instantaneous strain *reductions* γ_T' and θ_T' during the reverse m → t transformation are given by $\gamma_T'=\gamma_T/\sqrt{2}$ and $\theta_T'=\theta_T/2$, substantially smaller than the jumps of the t → m phase change. Clearly, such special relations can not have any basic significance, and are not to be regarded as predictions. Rather, they emphasize the likely need for more elaborate energy functionals in order to achieve consistency with the details of actual relations between direct and reverse transformation strains. Such experimental data for pressure cycling are not known to us.

Combined loading: hydrostatic stress and shear

It is convenient to work with the reduced energy function $\Phi-\Phi_0$, where Φ_0, defined as the potential energy of the fundamental tetragonal state (5) under pure hydrostatic stress, is given by

$$\Phi_0=\tfrac{1}{2}K\theta_0^2-\sigma\theta_0. \tag{10}$$

Then, (1), (2), (6) and (8) provide a nondimensional reduced energy Ψ that may be written as

$$\Psi(\theta,\gamma) \equiv \frac{\Phi-\Phi_0}{\Delta\sigma\theta_T} = \frac{\omega}{2}\left[\frac{\theta-\theta_0}{\theta_T} - \left(\frac{\gamma}{\gamma_T}\right)^2\right]^2 - \left(\frac{\sigma-\sigma_c}{\Delta\sigma}\right)\left(\frac{\gamma}{\gamma_T}\right)^2 - 2\left(\frac{\gamma}{\gamma_T}\right)^4 + \frac{4}{3}\left(\frac{\gamma}{\gamma_T}\right)^6 - \left(\frac{\tau\gamma_T}{\Delta\sigma\theta_T}\right)\frac{\gamma}{\gamma_T} \quad (11)$$

where

$$\omega = \frac{K\theta_T}{\Delta\sigma}. \quad (12)$$

The equilibrium equations $(\partial\Psi/\partial\theta) = (\partial\Psi/\partial\gamma) = 0$ give

$$\frac{\theta-\theta_0}{\theta_T} = \left(\frac{\gamma}{\gamma_T}\right)^2 \quad (13a)$$

$$\left[\frac{\sigma-\sigma_c}{\Delta\sigma}\right]\frac{\gamma}{\gamma_T} = 4\left[-\left(\frac{\gamma}{\gamma_T}\right)^2 + \left(\frac{\gamma}{\gamma_T}\right)^4\right]\frac{\gamma}{\gamma_T} - \frac{z}{2} \quad (13b)$$

where we have introduced the nondimensional shear stress parameter

$$z \equiv \left(\frac{\tau}{\Delta\sigma}\right)\left(\frac{\gamma_T}{\theta_T}\right). \quad (13c)$$

[The θ–γ relation (13a) is the same as it was for $\tau = 0$.] Equations (13) provide the dashed curves in Figs 5(a) and (b), which show how the application of a constant shear stress, represented by several values of z, affects the relations between hydrostatic stress and strain. The important thing to note is that in the presence of shear the t → m phase transformation under increasing σ is no longer associated with a *bifurcation* instability, as it was for $\tau = 0$. Instead, for a range of nonzero τs, the phase change reflects *limit-point* buckling at the local maximum in the σ–γ (or σ–θ) relation, and the critical stress σ_{max} for the t → m jump may be reduced substantially below σ_c by the presence of shear. For small values of τ, the snapping stress σ_{max} implied by (13) is given asymptotically by

$$\sigma_{max} \approx \sigma_c - 3(\Delta\sigma)^{1/3}\left(\frac{\tau\gamma_T}{2\theta_T}\right)^{2/3}. \quad (14)$$

The reverse m → t transformation stress σ_{min} is also lowered by shear stress (linearly for small τ), and the hysteresis $[\sigma_{max} - \sigma_{min}]$ is less than the original $\Delta\sigma$. Further, for sufficiently large values of shear stress, namely

$$\tau > \frac{48}{25}\sqrt{\frac{3}{10}}\,\frac{\theta_T\Delta\sigma}{\gamma_T} \quad (15)$$

the tetragonal-to-monoclinic transition under increasing σ becomes gradual, losing

its buckling character, and under reverse loading the trip back follows the same continuous path. All of this is qualitatively consistent with the buckling behavior of imperfection-sensitive structures, in which small initial displacements lead to catastrophic collapse at loads significantly lower than the critical bifurcation load.

Stress-space phase diagram

Equation (13b) implies that for $\sigma = \sigma_{\max}$ *or* $\sigma = \sigma_{\min}$, the variables γ, σ and τ must satisfy the relations

$$z \equiv \frac{\tau\gamma_T}{\Delta\sigma\theta_T} = 2\left(\frac{\gamma}{\gamma_T}\right)\left[-\frac{\sigma-\sigma_c}{\Delta\sigma} - 4\left(\frac{\gamma}{\gamma_T}\right)^2 + 4\left(\frac{\gamma}{\gamma_T}\right)^4\right] \tag{16a}$$

$$\frac{\sigma-\sigma_c}{\Delta\sigma} = -4\left[3\left(\frac{\gamma}{\gamma_T}\right)^2 - 5\left(\frac{\gamma}{\gamma_T}\right)^4\right] \tag{16b}$$

where (16b) follows from the condition, for fixed τ, $(\partial\sigma/\partial\gamma)_\tau = 0$ applied to (16a). Hence (16) provide a parametric representation, via γ/γ_T, for the t → m and m → t phase boundaries shown in Fig. 6. The range $0 \leqslant \gamma/\gamma_T \leqslant \sqrt{3/10}$ gives $\sigma_{\max}$ and the lower boundary, for $\sigma_{\min}$, corresponds to $\sqrt{3/10} \leqslant \gamma/\gamma_T \leqslant \sqrt{1/2}$. These curves intersect tangentially at the *critical point* $z = (48/25)\sqrt{3/10}$, $(\sigma-\sigma_c)/\Delta\sigma = -1.8$, corresponding to $(\partial^2\sigma/\partial\gamma^2)_\tau = 0$. Note the vertical slope at $\tau = 0$ of the t → m boundary, consistent with (15). (The reflection of these curves about the σ-axis provides the stress-space phase boundaries for $\tau < 0$.) The long arrows in Fig. 6 emphasize the directions of stress change that provoke t → m and m → t phase changes, and the distance between the two curves represents the hysteresis. However, the phase diagram is also valid for arbitrary stress paths in σ–τ stress space that cross the boundaries from the inside to the outside of the region they bound. Finally, we note that stress

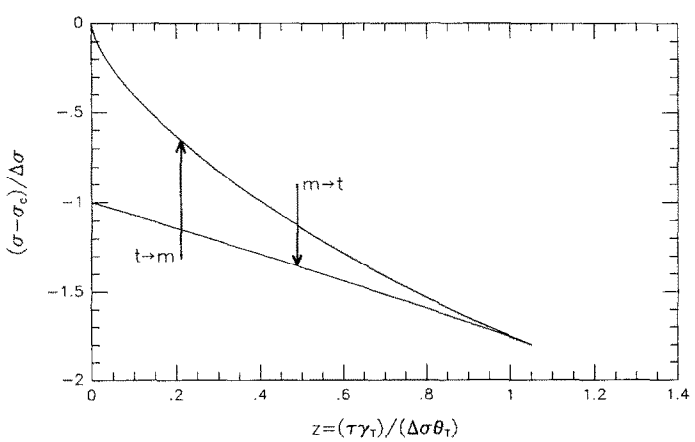

FIG. 6. Non-dimensional, isothermal phase diagram, showing combinations of hydrostatic stress σ and $\tau > 0$ for phase change; the arrows show directions of loading in stress-space for the tetragonal-to-monoclinic transformation and its reverse.

paths that remain outside this region induce only continuous strain changes, like those shown by the bottom curves of Fig. 5.

The t → m curve can be imagined analogous to a "yield" locus of plasticity theory, and then the associated jumps in θ and γ are like plastic strains. However, in conventional plasticity theory a "normality" rule constrains the plastic strain ratios. In our problem, the condition of normality means that at each point on the t → m phase boundary, the t → m jumps $\delta\theta$ and $\delta\gamma$, and increments $d\sigma$ and $d\tau$ *along* the curve, would have to satisfy the relation $\delta\theta\, d\sigma + \delta\gamma\, d\tau = 0$. This is clearly not so; indeed, at $\tau = 0$, normality would imply $\delta\theta = 0$!

It may be of interest to note that normality *would* hold if the phase jumps were arbitrarily required to occur (reversibly) on a phase boundary in σ–τ space corresponding to the Maxwell condition of equal potential energy in the two phases, rather than at the states of limit-point instability. Since the energy is

$$F = \int_{(0,0)}^{(\theta,\gamma)} (\sigma\, d\theta + \tau\, d\gamma) - \sigma\theta - \tau\gamma = \int_{(0,0)}^{(\sigma,\tau)} (\theta\, d\sigma + \gamma\, d\tau) \tag{17}$$

we have $dF = \theta\, d\sigma + \gamma\, d\tau$ along any curve in σ–τ space. The energy jump $\delta F = 0$ therefore implies $\delta[dF] = \delta\theta\, d\sigma + \delta\gamma\, d\tau = 0$ along the Maxwell locus. [This kind of argument was used by RICE (1971) to make normality plausible in plasticity.] However, we emphasize that there is no apparent reason to impose the Maxwell condition on martensitic phase changes that display stress hysteresis.

Monoclinic elastic moduli

A credibility check on our model can be made by calculating the predicted cross-compliance $d\gamma/d\sigma \equiv (\partial\gamma/\partial\sigma)_\tau$ of the stable monoclinic phase at zero pressure and shear, and comparing with available experimental data (NEVITT *et al.*, 1988) and atomic-theory estimates (COHEN *et al.*, 1988).

From (9b), the shear strain γ_0 at $\sigma = \tau = 0$ (and room temperature) is given by

$$\frac{\gamma_0}{\gamma_T} = \sqrt{\frac{1+\sqrt{1-\sigma_c/\Delta\sigma}}{2}} \tag{18}$$

and the *cross-compliance* $d\gamma/d\sigma$ follows from (9b) by differentiation. The reciprocal of this compliance is the monoclinic cross-modulus given by

$$\left(\frac{d\gamma}{d\sigma}\right)^{-1} = 8\left(\frac{\Delta\sigma}{\gamma_0}\right)\left(\frac{\gamma_0}{\gamma_T}\right)^2\left[-1+2\left(\frac{\gamma_0}{\gamma_T}\right)^2\right] \tag{19a}$$

$$= 8\left(\frac{\Delta\sigma}{\gamma_0}\right)\left(\frac{\gamma_0}{\gamma_T}\right)^2\sqrt{1-\frac{\sigma_c}{\Delta\sigma}}. \tag{19b}$$

This is the slope of the σ–γ curve (Fig. 4) at $\sigma = 0$, $\gamma = \gamma_0$. Similarly, by differentiation of (13), we get the monoclinic shear modulus at $\sigma = \tau = 0$ as

$$\left(\frac{d\gamma}{d\tau}\right)^{-1} = 16\left(\frac{\Delta\sigma}{\gamma_0}\right)\left(\frac{\theta_T}{\gamma_T}\right)\left(\frac{\gamma_0}{\gamma_T}\right)^3\sqrt{1-\frac{\sigma_c}{\Delta\sigma}}. \tag{20}$$

The *sign* of the predicted value of $(d\gamma/d\sigma)^{-1}$ is of particular interest. Our model says it is positive, which means that incremental hydrostatic tension applied to room-temperature, monoclinic zirconia should *increase* the shear angle γ defined in Figs 1 and 2. Careful attention to sign convention is clearly crucial in the assessment of this prediction vis-à-vis the measurements of Nevitt *et al.* and the atomic calculations of Cohen *et al.* Telephone communication with both Nevitt and Cohen has confirmed that they used conventional monoclinic axes (NYE, 1957), for which the β-angle between the a and c axes (Fig. 1) is *greater* than 90°, whereas we adopted the twinned configuration having an acute angle between the a and c axes. This means that we have to change the signs of their reported tension-shear cross-compliances when we use them to make comparisons with the predictions of (19). (More precisely, in terms of the standard crystallographic compliances S_{ij}, our $d\gamma/d\sigma$ is equal to $[-S_{15}-S_{25}-S_{35}]$.)

Guided by the measurements of BLOCK *et al.* (1985) for room-temperature zirconia we assume $\sigma_c = -2.8$ GPa and $\Delta\sigma = 0.6$ GPa in (18) to get $\gamma_0/\gamma_T = 1.30$. Although the transformation strain γ_T has usually been presumed to be equal to about 0.16, this is evidently based on the value of $(\beta-\pi/2)$, where $\beta \approx 99°$ is the reported magnitude of the angular lattice parameter of monoclinic zirconia at zero pressure and room temperature (GREEN *et al.*, 1989). Hence it is more appropriate to use 0.16 as the value of γ_0, rather than γ_T, in (19) and (20). A room-temperature value of θ_T is not well established, but we will evaluate (20) using the assumption $\gamma_T/\theta_T = 4$. This is consistent with lattice-parameter data quoted by GREEN *et al.* (1989, p. 220) for monoclinic ZrO_2 at 956°C and tetragonal ZrO_2 at 1152°C, which indicate $\theta_T \approx 0.03$, rather than the usually assumed value 0.04.

Table 1 shows the magnitudes of $(d\gamma/d\sigma)^{-1}$ and $(d\gamma/d\tau)^{-1}$ thereby given by (19) and (20), together with the values (for our coordinate system) derived from the measurements of Nevitt *et al.* and the atomic estimates of Cohen *et al.* The two sets of numbers in the last column correspond to two different atomic structures that were assumed by Cohen *et al.* for monoclinic zirconia.

Not too much significance should be attached to the absolute magnitudes of our numbers, because our model is so primitive, but the difference in sign between our result for the cross-modulus and Nevitt's experimental value is disappointing, because it is hard to see how our model could easily be modified to change the sign of $d\gamma/d\sigma$. Of course, the same sign difference between the Nevitt and Cohen results do suggest

TABLE 1. *Monoclinic moduli (GPa)* ($\sigma_c = -2.8$ GPa, $\Delta\sigma = 0.6$ GPa, $\gamma_0 = 0.16$, $\gamma_T/\theta_T = 4$)

Modulus	Equations (18)–(20)	Nevitt *et al.* (1988)	Cohen *et al.* (1988)
$(d\gamma/d\sigma)^{-1}$	121	−680	400, 260
$(d\gamma/d\tau)^{-1}$	78	65	90, 64

that final judgement may be premature. In this connection, we have scrutinized the elastic constants tabulated by SIMMONS and WANG (1971) for 21 different monoclinic materials, and we find that $d\gamma/d\sigma$ is positive for 12 of these, and negative for the rest. Perhaps our model and variants thereof could make sense only for some kinds of monoclinic materials and not others. (Also, we remain uneasy about the consistency of the sign conventions for monoclinic crystals used by various authors.)

Although our zirconia model has failed to pass the experimental credibility check we sought, we will stay with it a little longer, and explore some of its consequences concerning phase changes of *inclusions* from tetragonal to monoclinic, and back.

Elastically constrained crystals

We contemplate next an isolated, single tetragonal crystal embedded in an infinite matrix of non-transforming, isotropic, linearly elastic material, and seek to determine critical combinations of stress at infinity that will cause its transformation to a monoclinic phase. We restrict ourselves to the application of just two stress types at infinity, namely hydrostatic stress σ^∞ and a single shear stress τ^∞, the latter aligned with the a–c axes (Fig. 3) of the tetragonal inclusion. In this exploratory study, we will make some simplifying assumptions, as follows:

(i) the inclusion will be assumed to be spherical;

(ii) strains will be assumed homogeneous in the inclusion; specifically, twinning will be presumed not to occur;

(iii) we will continue to apply the single crystal relations (9a) and (13) connecting σ, τ, θ and γ to the inclusion, with σ reinterpreted as the *mean* normal stress. This represents an extra simplifying assumption, because the constrained crystal will suffer stress states that are more complex than the combination of pure hydrostatic loading and simple shear which we contemplated in our study of the unconstrained crystal;

(iv) the bulk modulus of the matrix will be set equal to the tetragonal bulk modulus K of the inclusion.

Assumption (ii) is drastic. Constrained tetragonal zirconia inclusions generally *do* display multiple twinned monoclinic bands when they transform. It seems, nevertheless, worthwhile to pursue the idealized constrained-crystal model we have set, to see how the calculations go, in preparation for the considerably more sophisticated analysis that would be needed to take twinning into account; and to gain some insight into the magnitudes of stresses and strains that would be involved in a hypothetical twin-free transformation.

The exact Eshelby–Hill relations (ESHELBY, 1957; HILL, 1965) for a homogeneous spherical inclusion can be written as

$$\begin{cases} \sigma^\infty - \sigma = K(\alpha^{-1} - 1)(\theta - \theta^\infty) \\ \tau^\infty - \tau = G_M(\beta^{-1} - 1)(\gamma - \gamma^\infty) \end{cases} \tag{21}$$

in terms of the bulk modulus K and shear modulus G_M of the matrix, and the Eshelby parameters

$$\alpha = \frac{1+\nu}{3(1-\nu)}, \quad \beta = \frac{2(4-5\nu)}{15(1-\nu)}. \tag{22a}$$

The strains at infinity are $\theta^\infty = \sigma^\infty/K$ and $\gamma^\infty = \tau^\infty/K$. With $G_M = K[3(1-2\nu)]/[2(1-\nu)]$ (21), together with the inclusion relations (13) may be used to eliminate σ and τ, and get the connections

$$\frac{\theta-\theta^\infty}{\theta_T} = \alpha\left(\frac{\gamma}{\gamma_T}\right)^2 \tag{22b}$$

$$\left[\frac{\sigma^\infty-\sigma_c}{\Delta\sigma} - \lambda\omega(\gamma_T/\theta_T)^2\right]\frac{\gamma}{\gamma_T} = 4\left[-c\left(\frac{\gamma}{\gamma_T}\right)^2 + \left(\frac{\gamma}{\gamma_T}\right)^4\right]\frac{\gamma}{\gamma_T} - \frac{(\tau^\infty/\Delta\sigma)(\gamma_T/\theta_T)}{2\beta} \tag{22c}$$

where

$$\lambda = \frac{3(1-2\nu)(7-5\nu)}{4(1+\nu)(4-5\nu)} \tag{23}$$

and

$$c = 1-\omega(1-\alpha)/4. \tag{24}$$

It now follows from (22b) that for $\tau^\infty = 0$, the tetragonal inclusion strains remain equal to $\theta = \theta^\infty$ and $\gamma = 0$ until σ^∞ reaches the bifurcation stress

$$\begin{aligned}\sigma_c^\infty &= \sigma_c + \lambda\omega(\gamma_T/\theta_T)^2 \\ &= \sigma_c + \lambda K\gamma_T^2/\theta_T.\end{aligned} \tag{25}$$

The inclusion strains will then have finite jumps *only* if $c > 0$, with magnitudes

$$\bar{\gamma}_T = \sqrt{c}\gamma_T, \quad \bar{\theta}_T = \alpha c\theta_T. \tag{26}$$

During reverse loading, the jump back to the tetragonal state will occur at $\sigma^\infty = \sigma_c^\infty - \Delta\sigma^\infty$, where

$$\Delta\sigma^\infty = c^2(\Delta\sigma) \tag{27}$$

is the hysteresis in σ^∞. The relations (22b,c) may now be rewritten to look very much like those in (13) for the unconstrained crystal, as follows:

$$\frac{\theta-\theta^\infty}{\bar{\theta}_T} = \left(\frac{\gamma}{\bar{\gamma}_T}\right)^2 \tag{28a}$$

$$\left[\frac{\sigma^\infty-\sigma_c^\infty}{\Delta\sigma^\infty}\right]\frac{\gamma}{\bar{\gamma}_T} = 4\left[-\left(\frac{\gamma}{\bar{\gamma}_T}\right)^2 + \left(\frac{\gamma}{\bar{\gamma}_T}\right)^4\right]\frac{\gamma}{\gamma_T} - \frac{\bar{z}}{2} \tag{28b}$$

where

$$\bar{z} \equiv \frac{\alpha}{\beta}\left(\frac{\tau^\infty}{\Delta\sigma^\infty}\right)\left(\frac{\bar{\gamma}_T}{\bar{\theta}_T}\right). \tag{29}$$

Accordingly, for $c > 0$, all of the results plotted in Figs 5–6 become applicable to the constrained crystal, simply by substituting σ^∞, σ_c^∞, $\Delta\sigma^\infty$ for σ, σ_c and $\Delta\sigma$, respectively, and replacing γ_T, θ_T and z by $\bar{\gamma}_T$, $\bar{\theta}_T$ and $\bar{z}$. For the special case $\nu = 0.2$, (22) give $\alpha = \beta = 0.5$, and the analogy between (13)–(14) and (28)–(29) becomes perfect. For this choice of ν, we get $\lambda = 3/8$ and $c = 1 - \omega/8$.

For $c < 0$, (22) show that even with $\tau^\infty = 0$ the inclusion would undergo a smooth transition to a monoclinic-like state as the remote hydrostatic tension is increased beyond its critical value. This corresponds to the case called "subcritical" by BUDIANSKY *et al.* (1983); their "supercritical" case, in which the constrained inclusion transforms abruptly at a critical stress, corresponds to $c > 0$.

A rough estimate of σ_c^∞ via (25), with $\lambda = 3/8$, $K = 150$ GPa, $\sigma_c = -3$ GPa, $\gamma_T = 0.12$, and $\theta_T = 0.03$, gives $\sigma_c^\infty = 24$ GPa. This seems much too high; working backwards from measured toughnesses of transformation-toughened materials suggests values of σ_c^∞ around 1/2 GPa. Some reduction of the elastic constraint on inclusions can be attributed to inclusion interaction, but the chief culprit invalidating the calculation of σ_c^∞ must be twinning. Finally, we note that for $\nu = 0.2$, the supercritical transformation criterion $c > 0$ requires $\omega = K\theta_T/\Delta\sigma < 8$; with $\Delta\sigma = 0.6$, we get the estimate $\omega = 10$—too high for supercriticality.

Twin bands and twinning

There are at least two distinct ways in which twinned configurations could occur in transforming crystals (CHEN and CHIAO, 1983), thereby invalidating our calculations. First of all, even an unconstrained tetragonal crystal can be expected to suffer twinning as it transforms to the monoclinic state, as a consequence of habit-plane compatibility requirements when a phase-change interface sweeps across the crystal (WAYMAN, 1964). Second, minimum-energy requirements associated with the phase change of an elastically constrained embedded single crystal may induce bands of monoclinic variants, as has generally been observed in all but very small inclusions. At least qualitatively, this kind of twin-band development, and the dependence of the number of twin bands on crystal size, may be analysed (e.g. EVANS *et al.*, 1981; KOHN and MULLER, 1992) on the basis of a trade-off between the reduced elastic strain energy provoked by multiply twinned configurations of transforming embedded inclusions and the band interface surface energies. A quantitative mechanical analysis for zirconia of these twinning issues and their interactions, in the spirit of the present approach, remains to be executed. Not least of the difficulties in such a task is the stipulation of the required twin-band interface energies, the magnitudes of which are not known.

CONCLUDING REMARKS

Subject to the admittedly drastic simplification of permitting only homogeneous states in both constrained and unconstrained crystals, we have presented a model for tetragonal-to-monoclinic transformation in zirconia, and the reverse phase change, under a simple state of combined hydrostatic tension σ and shear τ. The nature of the

combined σ–τ stress conditions for phase change has been explored, albeit speculatively, as have several other implications of the model. Similar studies involving more complex stress states of loading can be undertaken, and the more challenging problem of incorporating twinning effects remains to be met.

ACKNOWLEDGEMENTS

We are grateful for instructive comments by Professor Arthur Heuer concerning the essential role of twinning in zirconia phase transformation. This work was supported in part by the National Science Foundation under a Materials Research Laboratory grant (DMR-89-20490), in part by a DARPA University Research Initiative grant (Subagreement P.O. No. VB38639-0 with the University of California, Santa Barbara, ONR Prime Contract 00014-86-K-0753), by the Division of Applied Sciences, Harvard University, and by the Department of Aerospace Engineering and Mechanics, University of Minnesota.

REFERENCES

AMAZIGO, J. C. and BUDIANSKY, B. (1988) Steady-state crack growth in supercritically transforming materials. *Int. J. Solids Struct.* **24,** 751–755.

ARASHI, H., SKIMOMURA, O., YAGI, T., AKIMOTO, S. and KUDOK, Y. (1988) P–T Phase diagram of ZrO_2 determined by *in situ* X-ray diffraction, measurements at high pressures and high temperatures. In *Advances in Ceramics*, Vol. 24, pp. 493–500. Science and Technology of Zirconia III, Am. Ceram. Soc., Westerville, OH.

BLOCK, S., DA JORNADA, J. A. H. and PIERMARINI, G. J. (1985) Pressure–temperature phase diagrams of Zirconia. *J. Am. Ceram. Soc.* **68,** 497–499.

BUDIANSKY, B. (1974) Theory of buckling and post-buckling behavior of elastic structures. *Advances in Applied Mechanics*, Vol. 14, pp. 1–65. Academic Press, New York.

BUDIANSKY, B., HUTCHINSON, J. W. and LAMBROPOULOS, J. C. (1983) Continuum theory of dilatant transformation toughening materials. *Int. J. Solids Struct.* **19,** 337–356.

CHAN, S. K. (1988) The polymorphic transformations of Zirconia. *Physica B* **150,** 212–222.

CHEN, I.-W. and CHIAO, Y.-H. (1983) Martensitic nucleation in ZrO_2. *Acta Metall.* **31,** 1627–1638.

CHEN, I.-W. and REYES MOREL, P. E. (1986) Implications of transformation plasticity in ZrO_2-containing ceramics: I, shear and dilatation effects. *J. Am. Ceram. Soc.* **69,** 181–189.

CHEN, I.-W. and REYES MOREL, P. E. (1987) Transformation plasticity and transformation toughening in Mg–PSZ and Ce–TZP. *Mater. Res. Soc. Symp. Proc.* **78,** 75–78.

CHIAO, Y.-H. and CHEN, I.-W. (1990) Martensitic growth in ZrO_2. *Acta Metall. Mater.* **38,** 1163–1174.

COHEN, R. E., MEHL, M. J. and BOYER, L. L. (1988) Phase transitions and elasticity in Zirconia. *Physica B* **150,** 1–9.

ESHELBY, J. D. (1957) The determination of the elastic field of an ellipsoidal inclusion, and related problems. *Proc. R. Soc.* **A241,** 376–396.

EVANS, A. G., BURLINGAME, N., RORY, M. and KRIVEN, W. M. (1981) Martensitic transformations in zirconia—particle size effects and toughening. *Acta Metall.* **29,** 447–456.

EVANS, A. G. and CANNON, R. M. (1986) Toughening of brittle solids by martensitic transformations. *Acta Metall.* **34,** 761–800.

EVANS, A. G. and HEUER, A. H. (1980) Review: transformation toughening in ceramics: martensitic transformations in crack-tip stress fields. *J. Am. Ceram. Soc.* **63,** 241–248.

GARVIE, R. C., HANNINK, R. H. J. and PASCOE, R. T. (1975) Ceramic steel. *Nature* **258,** 695–708.

GREEN, D. J., HANNINK, R. H. J. and SWAIN, M. V. (1989) *Transformation Toughening of Ceramics*. CRC Press, U.S.A.

HILL, R. (1965) Continuous micro-mechanics of elastoplastic polycrystals. *J. Mech. Phys. Solids* **13,** 89–101.

KOHN, R. V. and MULLER, S. (1992) Surface energy and microstructure. In *Shape-Memory Materials and Phenomena-Fundamental Aspects and Applications* (ed. C. T. LIU, M. WUTTIG, K. OTSUKA and H. KUNSMAN), Vol. 246, pp. 19–23. MRS, U.S.A.

KOITER, W. T. (1945) On the stability of elastic equilibrium (in Dutch). Thesis, Delft Univ., H. J. Paris, Amsterdam; English Transl. (a) NASA TT-F10, 833 (1967), (b) AFFDL-TR-70-25 (1970).

LAMBROPOULOS, J. C. (1986) Shear, shape and orientation effects in transformation toughening. *Int. J. Solids Struct.* **22,** 1083–1106.

MCMEEKING, R. M. and EVANS, A. G. (1982) Mechanics of transformation toughening in brittle materials. *J. Am. Ceram. Soc.* **65,** 242–246.

NEVITT, M. V., CHAN, S. K., LIU, J. Z., GRIMSDITCH, H. H. and FANG, Y. (1988) The elastic properties of monoclinic ZrO_2. *Physica B* **150,** 230–233.

NYE, J. F. (1957) *Physical Properties of Crystals*. Oxford University Press, London.

RICE, J. R. (1971) Inelastic constitutive relations for solids: an internal variable theory and its application to metal plasticity. *J. Mech. Phys. Solids* **19,** 433–455.

ROSE, L. R. F. (1986) The size of the transformed zone during steady-state cracking in transformation toughened materials. *J. Mech. Phys. Solids* **34,** 609–616.

RÜHLE, M. and EVANS, A. G. (1989) High toughness ceramics and ceramic composites. *Prog. Mater. Sci.* **33,** 85–167.

SIMMONS, G. and WANG, H. (1971) *Single Crystal Elastic Constants and Calculated Aggregate Properties: A Handbook*. MIT Press, Cambridge, MA.

STUMP, D. M. (1991) The role of shear stresses and shear strains in transformation-toughening. *Phil. Mag.* **A64,** 879–902.

STUMP, D. M. and BUDIANSKY, B. (1989a) Crack growth resistance in transformation toughened ceramics. *Int. J. Solids Struct.* **25,** 635–646.

STUMP, D. M. and BUDIANSKY, B. (1989b) Finite cracks in transformation-toughened ceramics. *Acta Metall.* **37,** 3297–3304.

SUN, Q. P., HUANG, Y., YU, S. P. and HWANG, K. C. (1990) Toughening analysis of Mode I and Mode III cracks in PSZ and TPZ ceramics, preprint.

WAYMAN, C. M. (1964) *Introduction to the Crystallography of Martensitic Transformations*. Macmillan, New York.